Coral hosts actively accumulate inorganic carbon for Symbiodiniaceae to maintain symbiotic relationships

Boya Zhang[1], Si Tang[1], Lu Liu[1], Meiting Xu[2], Yaqing Liu[1], Jianming Zhu[1], Weimin Xiao[3], Hongsheng Bi[4], Jin Zhou[1], Mark C. Benfield[5] & Zhonghua Cai[1,6,*]

[1]Shenzhen Public Platform for Screening and Application of Marine Microbial Resources, Tsinghua Shenzhen International Graduate School, Shenzhen 518055 Guangdong Province, PR China.

[2]School of Environment, Harbin Institute of Technology, Harbin 150090 Heilongjiang Province, PR China.

[3]Shenzhen Academy of Metrology and Quality Inspection, Shenzhen 518109 Guangdong Province, PR China.

[4]Chesapeake Biological Laboratory, University of Maryland Center for Environmental Science, Solomons, MD, USA.

[5]College of the Coast and Environment Department of Oceanography and Coastal Sciences, Louisiana State University, Baton Rouge, LA 70803, USA.

[6]Technology Innovation Center for Marine Ecology and Human Factor Assessment of Natural Resources Ministry, Tsinghua Shenzhen International Graduate School, Shenzhen 518055 Guangdong Province, PR China.

[*]Corresponding author: Zhonghua Cai (caizh@sz.tsinghua.edu.cn)

Abstract

High primary productivity of coral reefs is widely attributed to the mutualistic symbiosis between coral hosts and their microalgal partners (Symbiodiniaceae). Although the mechanisms maintaining this symbiosis have been considerable investigated, how the symbiont microalgae within coral get sufficient CO_2 for photosynthesis still remains inadquately explored. Here, we hypothesized that corals may actively accumulate dissolved inorganic carbon (DIC) for microalgae to maintain the symbiosis. Carbon (HCO_3^- and glucose) supply and consumption were evaluated in the scleractinian coral (*Goniopora lobata*) and its symbiont under light and dark conditions. Results suggest that Symbiodiniaceae were high DIC consumers, requiring about 2-3 fold more DIC than free-living species. The corals were high DIC producers, with internal concentrations up to 4.2 fold higher than in the surrounding seawater. In the absence of microalgae utilization, the excess DIC they produced appeared detrimental to their own growth. Moreover, transcriptomic analysis identified several DIC enrichment pathways are evolved in corals to attact the Symbiodiniaceae, including CO_2 concentrating mechanisms, respiration, calcification and phosphoenolpyruvate carboxylase. Increased the CO_2 dosage in seawater may induce coral symbiosis bleaching. Our findings can deeper reveal on the mechanisms sustaining coral symbiosis, and may help to predict how some corals respond to DIC imbalance under climate changes.

Introduction

Coral reefs are recognized as having the highest levels of primary productivity (1500-5000 gC $m^{-2}a^{-1}$) in nature[1], while growing in shallow oligotrophic waters[2,3]. The high productivity of coral reefs is widely attributed to their symbiotic relationship with the microalgal zooxanthellae[4,5,6], recently reclassified as Symbiodiniaceae[7]. Within this mutualistic relationship, there exist complicated and intimate resource exchanges between these two partners. For instance, the microalgal symbionts can derive nutrients like inorganic carbon (C), nitrogen (N) and phosphorus (P) from corals[8,9,10]. In return, the corals can also acquire food such as glucose, amino acids, lipids, etc. by absorbing microalgal photosynthesis products even digesting parts of the symbiont population[11,12,13,14].

From a stoichiometric perspective, coral's high productivity requires a high organic carbon supply, this means that an active photosynthesis of the microalgal symbiont should be working. Functioning photosynthesis of Symbiodiniaceae requires relatively high level of dissolved inorganic carbon (DIC, CO_2, and HCO_3^- and CO_3^{2-}) supply, as Symbiodiniaceae posseses type II ribulose-1,5-bisphosphate carboxylase/oxygenase (Rubisco, the key enzyme for carbon fixation), which has lower CO_2 affinity and specificity than type I Rubisco from other photoautotrophs[15,16]. Moreover, similar to other free-living microalgae that are usually challenged by insufficient DIC as CO_2 diffuses 10,000 times more slowly in water than in air[17], Symbiodiniaceae also faced this problem, which may be even worse as they inhabitated within the coral tissue and thus are physically separated from DIC in the surrounding seawater. It is therefore

62 very interesting to undertand how Symbiodiniaceae can meet their CO_2 requirement
63 for photosynthesis under such a situation. Due to the close and symbiotic relationship
64 between Symbiodiniaceae and the coral host, by now many efforts have been
65 invested to study DIC interactions between these two partners[18,19,20].
66 Understanding the DIC metabolism of the coral system is quite challenging because
67 DIC within coral tissue is involved in several processes: (1) CO_2 consumption by
68 microalgal photosynthesis; (2) CO_2 generation by the respiration of coral host and
69 Symbiodiniaceae; and (3) CO_2 generation and HCO_3^- consumption due to coral
70 calcification. Generally, besides HCO_3^- in seawater, coral respiration is deemed to be
71 the major contributor of photosynthetic CO_2[21,22], but different views have pointed out
72 these CO_2 will be rapidly transformed into HCO_3^- and used by the host itself for
73 calcification dependent on carbonic anhydrases (CAs) activities[23,24], and it is thus
74 believed that photosynthesis by microalgae and calcification by coral host compete
75 HCO_3^- in the tissue[25,26]. In contrast, others argued that these two processes are not in
76 a competitive relationship, instead host calcification can supply CO_2 for microalgal
77 photosynthesis, as well as recognizing that photosynthesis can drive rates of
78 calcification in the light[27,28,29]. More recently, researchers found that DIC
79 concentrations inside corals exceed ambient levels and confirmed the presence of
80 coral's CO_2 concentrating mechanisms (CCMs), nonetheless, the controversy
81 between symbiont photosynthesis and host calcification on internal-DIC competition
82 remains[24,30,31,32]. In addition, the productivity in Symbiodiniaceae may be
83 carbon-limited even multiple DIC supply pathways exist in stable symbiotic

84 systems[21,33,34]. The heterotrophic feeding of coral hosts also have a fairly important
85 impact on symbionts[35,36]. There is much more to be studied and understood about the
86 mechanisms supporting the complex coral symbiosis relationship.
87 Here, we explore the coral-microalgae symbiotic relationship focusing on the DIC
88 supplies in the symbiotic system and propose that coral hosts may actively
89 accumulate DIC for Symbiodiniaceae via respiration, calcification, CCMs, etc. To test
90 this hypothesis, the scleractinian coral (*Goniopora lobata*) was employed as a model,
91 which was widely distributed across the Indian and Pacific Oceans[37]. A series of
92 carbon source (HCO_3^- or glucose) utilization experiments were conducted under light
93 or dark regimes to determine the carbon consumption characteristics of the coral host
94 and symbionts, respectively. Transcriptomic analysis was then carried out to reveal
95 corresponding molecular traits. Finally, CO_2 enrichment experiments were performed
96 to simulate the impact of high external DIC concentrations on coral symbiosis.

97 **Results**

98 **DIC requirement in Symbiodiniaceae**

99 To determine the photosynthetic DIC requirements of the symbiotic microalgae, the
100 growth rates and carbon consumption rates of a monocultured Symbiodiniaceae
101 (*Symbiodinium* sp.), isolated from the *G. lobata*, were evaluated at 2 mM, 4 mM, and
102 8 mM dosages of $NaHCO_3$ over a period of 36 hours (Because N, P, etc. were still
103 available in this period, the microalgae were not limited by other nutrients). In general,
104 the symbiont showed the highest growth rate at 8 mM $NaHCO_3$, which reached 0.53
105 d^{-1} and was 2.08 and 1.34 times higher than that of cells grown with 2 mM and 4 mM

106 $NaHCO_3$, respectively (Fig. 1a, Two-way ANOVA, $F_{2,6} = 3.427$, $p < 0.05$). As expected,

107 faster-growing cells consumed more DIC. The average DIC consumption rates were

108 0.10 mM d^{-1}, 0.18 mM d^{-1}, and 0.26 mM d^{-1} corresponding to the 2 mM, 4 mM, and 8

109 mM $NaHCO_3$ treatments, respectively (Fig. 1b), whereas, the DIC concentration from

110 the blank control (without microalgae) remained almost unchanged (Fig. S1),

111 suggesting the decrease in DIC was caused by microalgal photosynthesis but not by

112 DIC run off. It was noteworthy that Symbiodiniaceae grown with different $NaHCO_3$

113 concentrations all showed a linear increase in biomass with DIC consumption,

114 suggesting that external DIC concentration is one of the limiting factors for its growth.

115 Meanwhile, based on the slope of linear regression (0.012 mol g^{-1} for all treatments,

116 Fig. 1b), it can be calculated that Symbiodiniaceae consume approximately 0.528 g of

117 CO_2 per gram of biomass growth, significantly higher than other free-living

118 microalgae[38,39,40]. These findings suggest that available DIC is an important limiting

119 factor for Symbiodiniaceae growth. Evidently, natural seawater with a DIC

120 concentration around 2 mM is a carbon-deficient environment for Symbiodiniaceae[41],

121 so whether the DIC concentrations inside coral tissues can meet microalgal

122 requirements and how this is achieved merits further investigation.

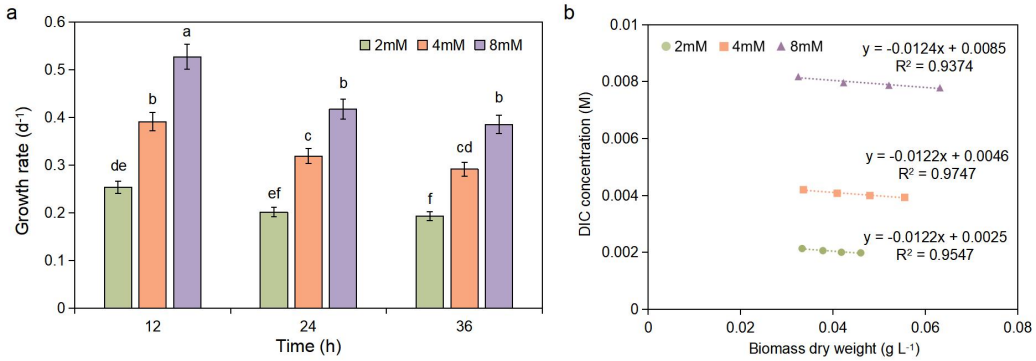

123

124 **Fig. 1: Growth rate and DIC consumption quantification of monocultured**

125 **Symbiodiniaceae at different carbon concentrations. a**, Growth rate of
126 Symbiodiniaceae over a period of 36 h. The graphs show the mean ± SD (n = 3).
127 Various letters above each bars indicate statistical significance ($p < 0.05$), calculated
128 by two-way ANOVA with Tukey's HSD posthoc analyses. **b**, Relationship between
129 carbon consumption and biomass growth of Symbiodiniaceae (n = 3). Slopes indicate
130 the carbon consumption for per gram of biomass growth. Data points are fitted with
131 exponential decay functions. R^2 values indicating the goodness of fits are shown.

132 **DIC production in the coral hosts**

133 To explore the carbon budget within the coral-Symbiodiniaceae system, carbon
134 supply experiments were performed under different light/dark regimes. Specifically,
135 we had four treatments, i.e., DG (Continuous darkness and glucose as the only
136 carbon source), DS (Continuous darkness and $NaHCO_3$ as the only carbon source),
137 LG (12 h/12 h light/dark and glucose as the only carbon source), and LS (12 h/12 h
138 light/dark and $NaHCO_3$ as the only carbon source). Here, CO_2 or HCO_3^- in the culture
139 medium was pre-purged by the method of Yellowlees et al.[42]

140 Over the 8-day experiment, visual changes (images), DIC and glucose utilization of
141 the corals were examined, respectively. Firstly, in the two treatments with glucose
142 addition (LG and DG), we found that the length of coral tentacle extension differed in
143 the light and dark, which were at most 1 cm longer in LG than in DG on day 4 (Fig. 2a).
144 With regard to glucose comsuption, interestingly, the glucose was consumed by coral
145 continuously in the light/dark regime, whereas corals grown in continual darkness
146 stopped glucose uptake since day 4, suggesting a possible critical role of microalgal

147 photosynthesis, which only occurs in the presence of light, in this process. At the end
148 of the experiment (day 8), corals grown in LG and DG consumed 0.0723 g L^{-1} and
149 0.0404 g L^{-1} glucose, respectively (Fig. 2c, $p<0.05$). Notably, from day 4 onwards the
150 internal-tissue glucose concentration of DG remained stable (approximately 0.0575 g
151 L^{-1}, Fig. 2e), but the DIC concentration continuously increased up to approximately
152 0.6009 g L^{-1}(Fig. 2c). In contrast, the internal-tissue glucose concentration of LG kept
153 increasing (from 0.0907 g L^{-1} to 0.1023 g L^{-1}, Fig. 2e), and the DIC concentration
154 gradually decreased (from 0.5632 g L^{-1} to 0.4297 g L^{-1}, Fig. 2c). These results
155 provided a good explanation for the morphological differences between corals in the
156 LG and DG treatments: that corals could continuously utilize glucose in the light due
157 to the consumption of internal-DIC by the symbiotic algae, whereas in the darkness,
158 corals could not take up glucose when their internal-DIC reached a certain threshold.
159 Secondly, in the $NaHCO_3$ groups (LS and DS), the difference in DIC uptake of corals
160 was also maximized between two groups on day 8 (LS=0.1180 g L^{-1}, DS=0.0213 g L^{-1},
161 $p<0.05$, Fig. 2b), suggesting DS absorbed few DIC in seawater. This is consistent with
162 coral visual changes, the length of coral tentacles extended up to 1.3 cm in LS on day
163 8, but hardly extended in DS during the experiment (Fig. 2a). Moreover, we detected
164 significantly higher DIC concentrations inside coral tissues compared to external
165 seawater in both groups, reaching a maximum of 4.2 and 1.6 times that of seawater
166 on day 4 in LS and DS, respectively (Fig. 2d). It is thus evident that DIC pools exist
167 within coral tissues no matter microalgal photosynthesis is functioning or not. Notably,
168 the enriched DIC within coral tissues in two glucose groups (LG and DG) were also

found above, and the higher DIC was not being released into seawater, because the DIC concentration in external seawater of these two groups remained stable (approximately 0.02 g L^{-1}, Fig. 2b).

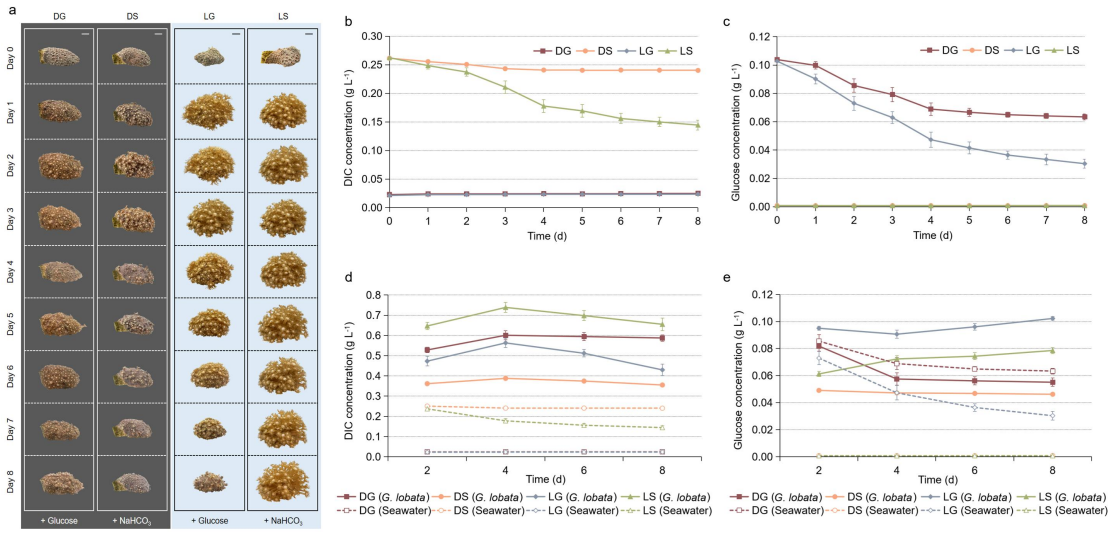

Fig. 2: Variation of coral morphology, DIC and glucose concentration in seawater and corals under different carbon sources and light conditions. a, The visual changes of representative replicate samples of corals exposed to DG, DS, LG, LS. Scale bars, 1 cm. **b**, DIC concentration in seawater. **c**, Glucose concentration in seawater. **d**, DIC concentration in corals. **e**, Glucose concentration in corals. Straight lines and dotted lines indicate corals and seawater, respectively. The graphs show the mean ± SD (n = 3). DG indicates continuous darkness and glucose as the only carbon source. DS indicates continuous darkness and $NaHCO_3$ as the only carbon source. LG indicates 12 h/12 h light/dark and glucose as the only carbon source. LS indicates 12 h/12 h light/dark and $NaHCO_3$ as the only carbon source.

Enzymatic activities and gene expression in carbon fixation

To resolve the origin of the high DIC pools in coral tissues, we analyzed the variance in the activity of carbon fixation enzymes of coral as a whole, and the differentially

186 expressed genes (DEGs) of the coral host and Symbiodiniaceae, respectively. Coral
187 grown in natural seawater (LS) was used as the control.
188 CAs, catalyze the interconversion of CO_2 and HCO_3^-, and indicators of CCMs, were
189 used to evaluate the DIC transformation of the coral symbiotic system. As to the
190 enzymatic activity of CAs, LS (42.16 U g^{-1} $prot^{-1}$) > LG (34.03 U g^{-1} $prot^{-1}$) > DG (27.31
191 U g^{-1} $prot^{-1}$) > DS (16.67 U g^{-1} $prot^{-1}$) at day 8 ($p < 0.05$, Fig. 3a) CAs activity in two
192 light groups (LS and LG) were gradually increased over culture period, but the two
193 dark groups (DS and DG) showed a tendency to rise and then fall, showing that the
194 CCMs of corals were affected by light. Subsequently, the expression of genes
195 encoding different types of CAs was found in both coral hosts and Symbiodiniaceae.
196 CAs are generally divided into α, β, and γ categories, with only α-CA in animals and all
197 three categories in higher plants, microalgae, and cyanobacteria[43,44]. Notably, in coral
198 hosts, seven α-CA genes were identified, and the DEGs of CA compared to LS were
199 down-regulated in both dark groups (DG and DS), but up-regulated in the light group
200 LG (Fig. 3d), indicating that their CCMs are associated with light. Moreover, in
201 Symbiodiniaceae, different CA subtypes and locations may perform different functions.
202 For example, the α-CA located in the cytoplasm and the β-CA1 in the chloroplasts
203 were also up-regulated under light conditions (Fig. 3d), while the β-CA2 located in the
204 cytoplasm was up-regulated in the dark groups (Fig. 3d).
205 In addition, we also identified an interesting pattern on the phosphoenolpyruvate
206 carboxylase (PEPCase) and phosphoenolpyruvate carboxykinase (PEPCKase), two
207 key enzymes for the biochemical CCMs, i.e., C_4 and crassulacean acid

208 metabolism (CAM)[45]. PEPCase catalyses the conversion of phosphoenolpyruvate
209 (PEP) to oxaloacetate and releases a CO_2 around Rubisco in C_4/CAM plants or
210 supplements malate to the TCA cycle directly in all organisms[46]. PEPCKase catalyses
211 the reverse pathway of PEPCase, converting oxaloacetate to PEP, and also plays a
212 key role in gluconeogenesis[47].
213 In terms of enzymatic activities, compared to LS, PEPCase was lower in the two
214 glucose-added groups and higher in DS (Fig. 3b), while PEPCKase was more active
215 in all treatments (especially in the two dark groups) (Fig. 3c). We attempted to explain
216 the possible reasons by DEGs. Results showed that the PEPC genes were not found
217 in coral hosts (Fig. 3e). Moreover, microalgal PEPC was mainly annotated as CAM
218 types and highly expressed in DS. PEPCK genes in host and Symbiodiniaceae were
219 generally up-regulated in the dark (Fig. 3e), which was consistent with the results of
220 PEPCKase activities (Fig. 3c), indicating that the limitation of light would have forced
221 both host and symbiont to synthesise glucose themselves. Notably, three sequences
222 were up-regulated in coral hosts under light conditions, especially in LS (Fig. 3e-LS in
223 red Gene ID), which was consistent with changes in PEPCKase activity at later stages
224 (Fig. 3c-LS).

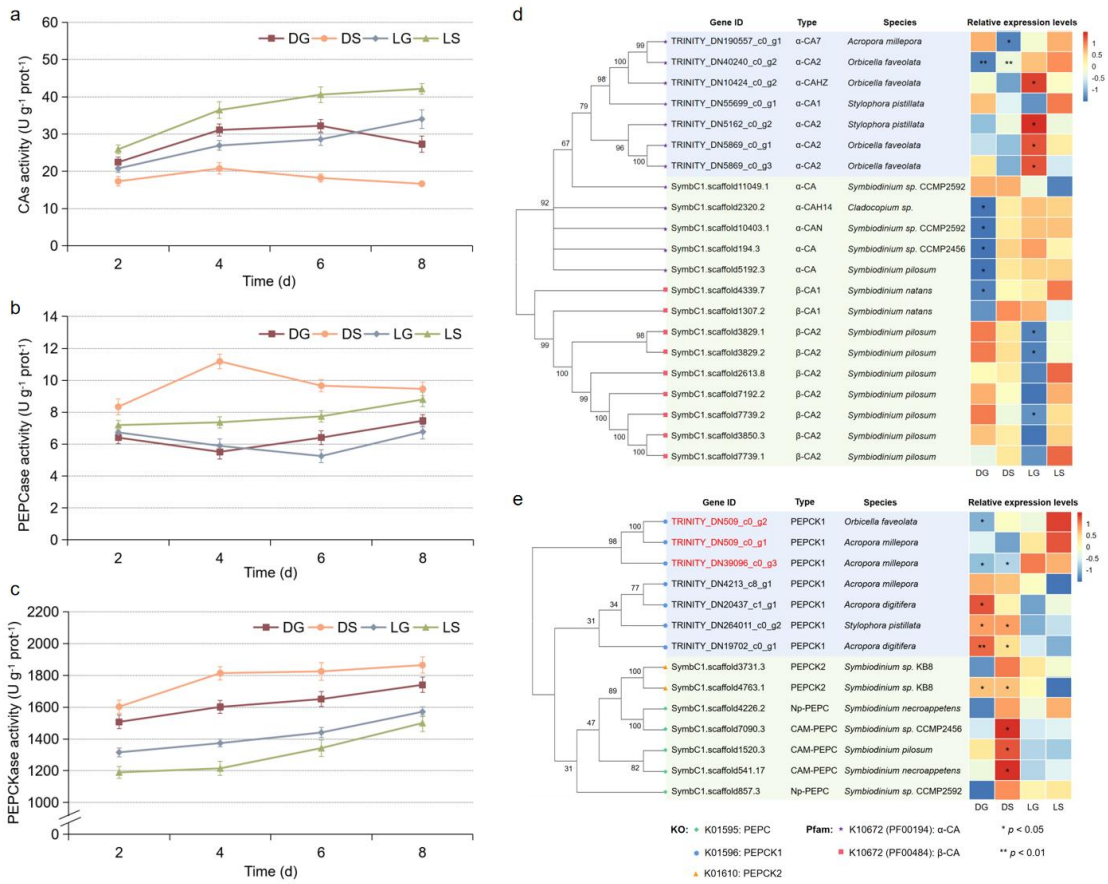

Fig. 3: CAs, PEPCase and PEPCKase activities and gene expressions in coral hosts and Symbiodiniaceae. a, CAs activity in corals. **b**, PEPCase activity in corals. **c**, PEPCKase activity in corals. **d**, Differential expression of CA genes in coral hosts and Symbiodiniaceae. **e**, Differential expression of PEPC and PEPCK genes in coral hosts and Symbiodiniaceae. The graphs show the mean ± SD (n = 3). The gene sequences selected in the figure are more than 50% similar to the corresponding gene sequences included in the KEGG database. The phylogenetic tree was drawn by MEGA software, and the values indicate the branch lengths. Gene ID indicates the ID number of the sequence in the transcriptome on the comparison, beginning with TRINITY for host and SymbC1.scaffold for Symbiodiniaceae. Type indicates the specific type of the enzyme encoded by the genes, which was obtained through the

237 KEGG module, Pfam, and Swissprot databases. Species indicate the similar species
238 to which the sequence was compared in the NCBI-NR database. Relative expression
239 levels are the log_2fc values of each treatment group compared to the control LS. P
240 indicates the significance of the difference between each treatment group and LS.

241 **Transcriptomic features of carbon metabolism of the coral host and**
242 **Symbiodiniaceae**

243 To explore the underlying mechanisms of DIC accumulation and transportation of the
244 symbiotic system on a molecular level, we investigated the carbon-involved
245 metabolisms in different coral treatments.

246 Glycolysis (purple arrows in Fig. 4c) and gluconeogenesis (red arrows in Fig. 4c)
247 pathways were used as indicators for glucose utilization activities. In Symbiodiniaceae,
248 compared to LS, all 9 genes annotated in glycolysis were down-regulated in DG, DS,
249 and LG, and the genes encoding three rate-limiting enzymes of glycolysis,
250 glucokinase (GLK) / hexokinase (HK), 6-phosphofructokinase (PFK),
251 and pyruvate kinase (PK)[48,49], were 2 out of 3 significantly down-regulated ($log_2fc > 1$,
252 $p < 0.05$) in DG. These lines of evidence pointed to external glucose being poorly
253 utilized by Symbiodiniaceae, as was also evident from its DEGs of photosynthesis
254 (Fig. S2). Meanwhile, the genes encoding the rate-limiting enzymes of
255 gluconeogenesis, PEPCK2 and fructose-1,6-bisphosphatase (FBP)[50], were
256 up-regulated in all three treatments, even significantly up-regulated ($log_2fc > 1$, $p <$
257 0.05) in DG, suggesting that it was consuming its own fatty acids to generate glucose.
258 In contrast, in coral hosts, out of 9 glycolysis-related DEGs, although 7 and 9 genes

259 were down-regulated in DG and DS, respectively, but 7 genes (including three
260 rate-limiting genes) were unchanged or up-regulated in the light group LG, which is in
261 accordance with the result from Fig. 2c-LG. Unsurprisingly, partial
262 gluconeogenesis-related genes (e.g., PEPCK1) of the host were up-regulated in DG,
263 DS and LG, probably due to the external glucose decrease in the post-culture period.
264 The TCA cycle (brown arrows in Fig. 4c), which is the central pathway for CO_2
265 production in aerobic organisms, was further explored. In Symbiodiniaceae,
266 compared to LS, the TCA cycle generally exhibited a decreased pattern, suggesting a
267 deceleration in respiration. Specifically, 9, 8 and 7 out of 13 genes annotated in the
268 TCA cycle were down-regulated in DG, DS, and LG, respectively. As to DEGs in coral
269 hosts, almost all genes were down-regulated in both dark treatment groups.
270 Conversely, 10 out of 14 TCA-related genes were unchanged or up-regulated in LG,
271 indicating that the host accelerated respiration to produce CO_2 in the light, combined
272 with the carbon consumption in coral tissues from Fig. 2d-LG. This CO_2 was likely to
273 be supplied to the microalgae.

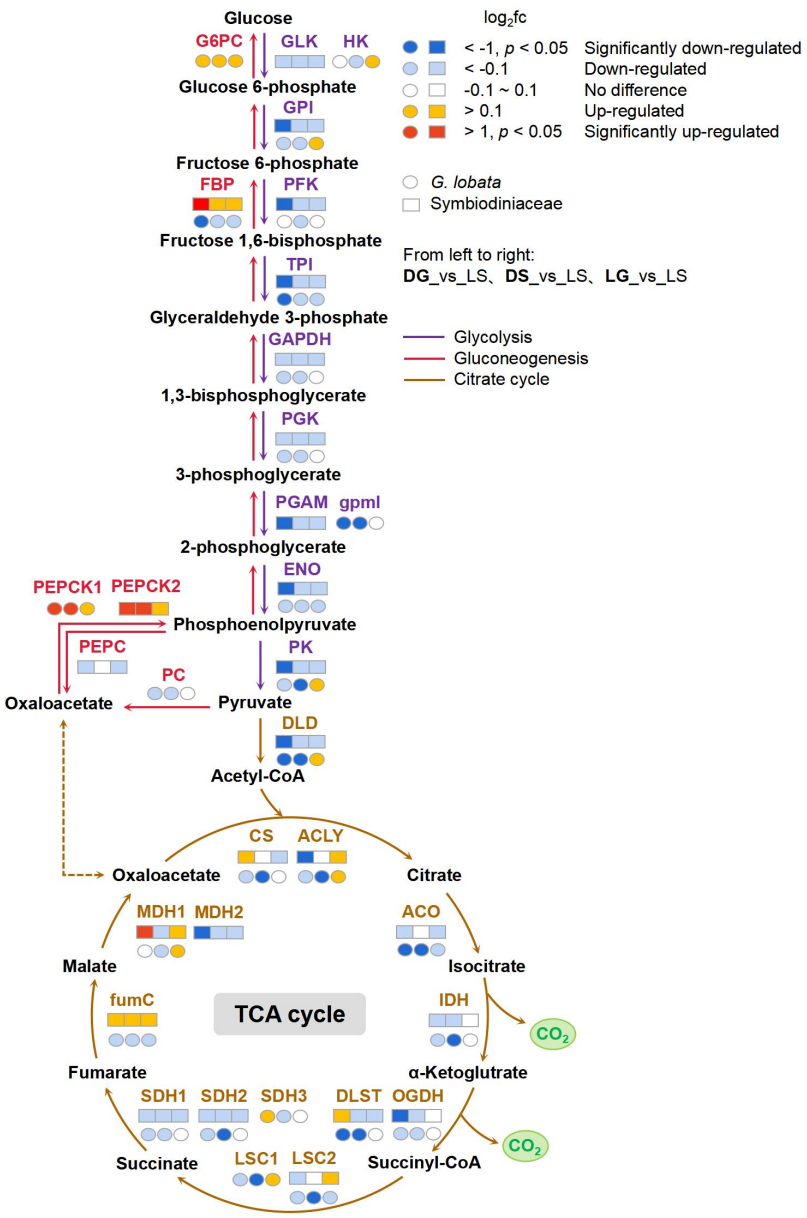

Fig. 4: DEGs of glycolysis, gluconeogenesis and TCA cycle genes in coral hosts and Symbiodiniaceae. The expression results of one sequence with the largest length of the transcriptome compared with the reference sequence of the KEGG database were selected for each gene in the figure. ○ indicates coral host, and □ indicates Symbiodiniaceae, where the colors indicate the log_2fc values of each treatment group compared to the control LS, from left to right once for DG, DS, and LG. Heatmap colors indicate relative expression levels, also the log_2fc values of each

282 treatment group compared with the control LS. *p* indicates the significance of the
283 difference between each treatment group and LS.
284 To further investigate whether CCMs from coral hosts acts on microalgal
285 photosynthesis or on its own growth, calcification, the coral-specific DIC metabolic
286 pathway central to coral physiology and health[51], was also analyzed. In general,
287 calcification-related genes displayed a decreased trend under dark conditions and an
288 increased trend under light conditions. Specifically, compared to the no-glucose
289 added group (LS), out of the 88 ion transporters DEGs responsible for active
290 transportation, i.e., calmodulin (CaM), calcium-binding proteins (CaBPs), Na^+/H^+
291 transports, HCO_3^- transports and CAs[52,53], 71 and 85 displayed a down-regulation in
292 DG and DS, respectively (Fig. 5a), for a total decrease of 59.31-log_2fc and
293 77.57-log_2fc (Fig. 5b). In contrast, the expression of DEGs in LG was 58 out of 88
294 genes unchanged or up-regulated (Fig. 5a), for a total increase of 20.05-log_2-fold (Fig.
295 5b), suggesting a correlation between coral calcification and light, rather than glucose.
296 Furthermore, galaxins, the sole skeletal organic matrix proteins definitively identified
297 in corals[54], continued to show a consistent down-regulation in DG and DS, while
298 exhibiting a 2.19-log_2-fold up-regulation in LG (Fig. 5b). The DEGs of other skeletal
299 organic matrix proteins associated with early calcification[55,56,57,58], were over 90%
300 down-regulated as well in two dark treatments, but 50% unchanged or up-regulated in
301 LG (Fig. 5a), which provides further evidence of the predominant influence of light
302 conditions, rather than carbon sources on calcification.

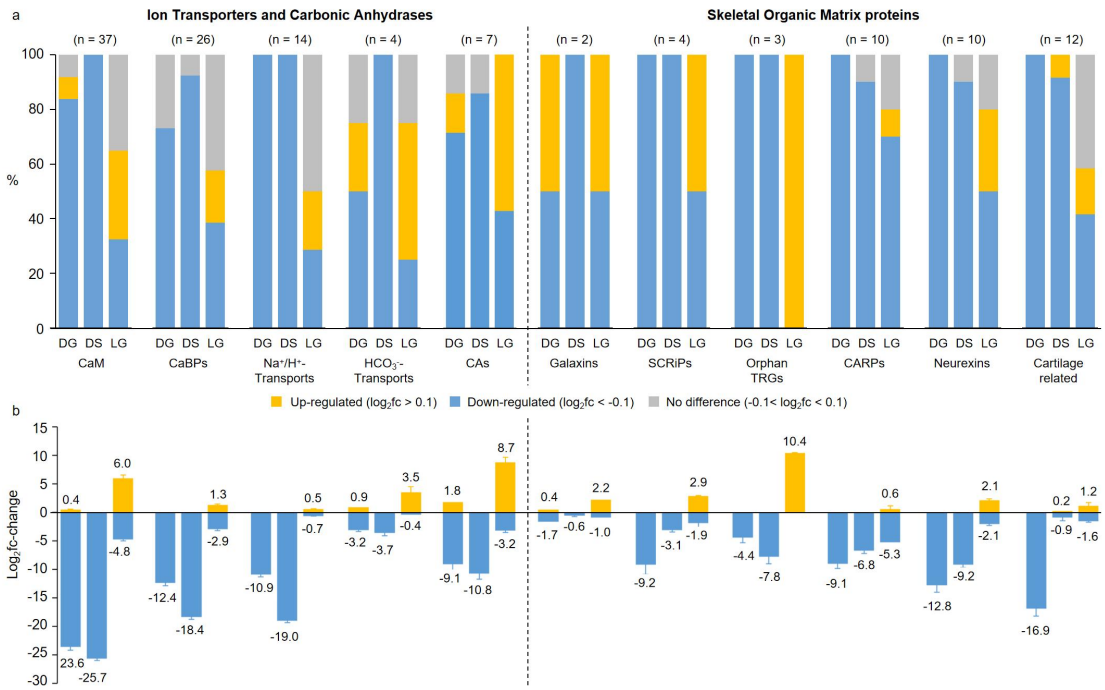

Fig. 5: Comparison of differential expression of genes related to calcification in coral hosts. a, Summary of changes on calcification genes in different categories (ion transporters, carbonic anhydrases, and skeletal organic matrix proteins) for DG, DS and LG treatments. Column colors indicate log_2fc values for each treatment group compared to control LS, with yellow up-regulated, blue down-regulated, and grey non-regulated. The total numbers of transcripts in each category are indicated above the corresponding bars. **b**, Summary of the corresponding mean log fold-change values for each of the classes of genes responding in part a. Actual fold-change values are indicated above or below each bar.

Elevated external CO_2 not low pH, induced detachment of Symbiodiniaceae

To examine the universality of our hypothesis that the corals may actively concentrate their internal DIC pool to favor symbiont photosynthesis as a primary evolutionary strategy for "retention" of symbiont microalgae, two scleractinian corals (*G. lobata* and model system *Acropora digitifera*) were cultured at three treatments: CO_2 group (1%

318 CO_2 mixture gas continuously aerated, pH = 7.0), HCl group (HCl added, pH = 7.0)
319 and control group (natural seawater, pH = 8.2). Results showed that in CO_2 group,
320 some corals lost more than half of their symbiont population, resulting in a bleached
321 appearance(Fig. 6ac). In the HCl group with the same pH, all corals maintained
322 normal symbiont populations (Fig. 6a), suggesting that higher external CO_2 levels
323 instead of other factors play an decisive role in the loss of the corals' symbiotic
324 microalgae. Specifically, the chlorophyll of *G. lobata* and *A. digitifera* decreased to
325 about 50% of that in the control groups on day 12 and day 3 in CO_2 groups (Fig. 6b).
326 We further explored whether the CO_2 solubility impacted on the microalgae loss. In
327 this study, the relationship between bubble diameter and CO_2 solubility was
328 determined by a Planktonscope and a total organic carbon analyzer (Fig. S3abc).
329 Results showed that smaller bubbles (d_{32} = 467 in group 2, Fig. S3abc) in the
330 microbubble plates led in higher CO_2 solubility (0.1703 g L^{-1} and 0.2000 g L^{-1} in group
331 2, Fig. 6c), and resulted in higher microalgal loss rates (59% and 84% in group 2, Fig.
332 6c). To determine whether stress impacted the coral bleaching, anti-oxidative
333 enzymes, i.e., superoxide dismutase (SODase) and catalase (CATase) activity were
334 detected in coral holobiont. Compared to natural conditions, the CO_2 group of two
335 corals had similar activities of SODase and CATase ($p > 0.05$), but the HCl group
336 significantly decreased the activities of the two enzymes (Fig. 6de, Two-way ANOVA,
337 $p < 0.05$). Meanwhile, the photosynthetic activity (Fv/Fm, Fig. S3de) of detached
338 Symbiodiniaceae in seawater was similar to that of the symbiotic Symbiodiniaceae
339 and possessed higher CAs activity (57.37 U g^{-1} $prot^{-1}$ and 46.32 U g^{-1} $prot^{-1}$, Fig. 6f) in

two corals, suggesting that the departure of Symbiodiniaceae from the host was not caused by stress response of excess CO_2 and they survived well outside of the corals.

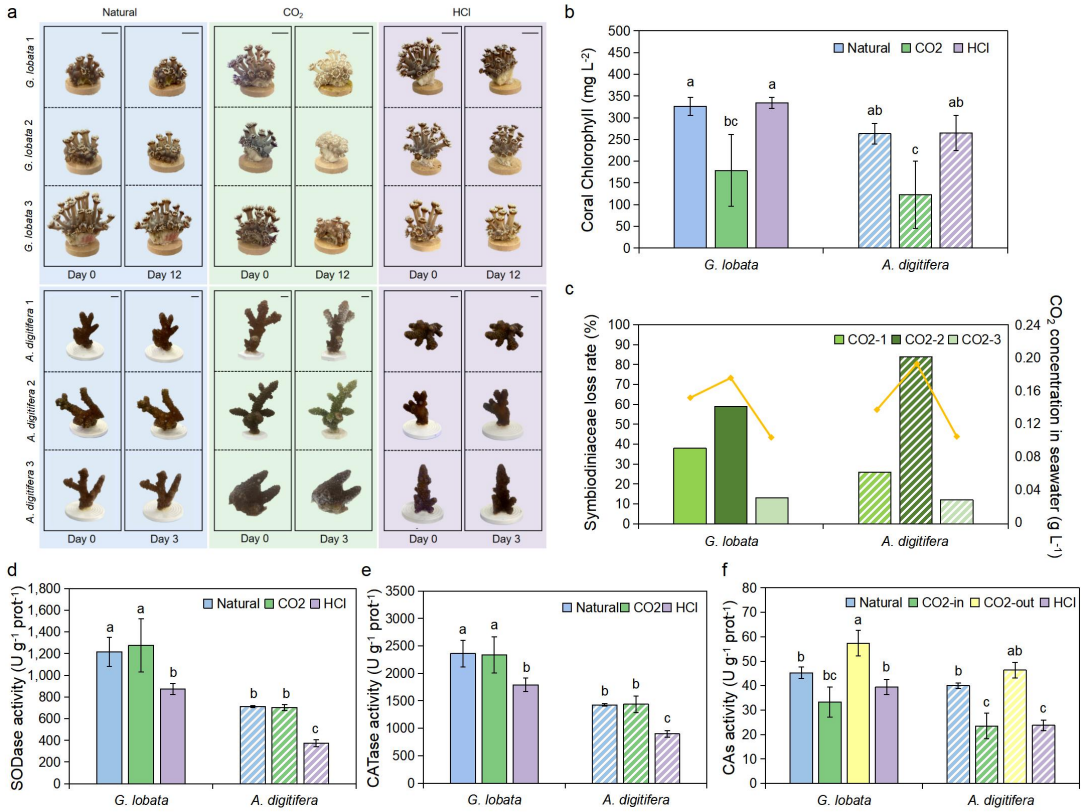

Fig. 6: Characterization of *G. lobata* and *A. digitifera* after external CO_2 and HCl addition. a, Visual changes of corals. **b**, Chlorophyll of corals on the last day. **c**, Symbiodiniaceae loss rates (bar charts) and CO_2 concentration in seawater (line graphs) of three CO_2 treatments on the last day. **d**, SODase activity of corals on the last day. **e**, CATase activity of corals on the last day. **f**, CAs activity of Symbiodiniaceae on the last day. Natural indicates natural seawater control group. CO_2 indicates 1% CO_2 mixture gas continuously aerated group. HCl indicates pH reduction with HCl addition group. The graphs show the mean ± SD (n = 3). Various letters above each bar indicate statistical significance ($p < 0.05$), calculated by

353 two-way ANOVA with Tukey's HSD posthoc analyses.

354 **Discussion**

355 Coral reefs are highly productive ecosystems that thrive in oligotrophic waters. The
356 success of this Darwinian paradox is mainly attributed to the successful symbiotic
357 relationship between the coral host and the symbiont Symbiodiniaceae[59,60]. Evidently,
358 efficient microalgal photosynthesis is paramount for this symbiotic system. However,
359 Symbiodiniaceae possess type II Rubisco enzymes characterised by a low CO_2
360 affinity, and they may also have higher CO_2 demands[15,16]. Here, we specifically
361 quantified the carbon requirements of isolated symbiotic microalgae, which consumed
362 about 0.528 g CO_2 per gram of biomass grown (Fig. 1b), suggesting that the
363 Symbiodiniaceae are "high consumers" of DIC. This is a far higher DIC demand than
364 that of some other free living microalgae. For example, *Haematococcus pluvialis*
365 consumes 0.308 g CO_2 for per gram of biomass growth[40], *Spirulina platensis* requires
366 0.256 g CO_2[38], and *Chlorella vulgaris* requires requires 0.218 g CO_2[39]. Obviously, the
367 symbiont microalgae must somehow cope with DIC limitation and perform
368 photosynthesis successfully and efficiently. It is reasonable that they may find high
369 DIC sites or habitats within coral tissue.

370 In this study, we employed *G. lobata* as model, and found that these scleractinian
371 corals are "high producers" of DIC, possessing a high internal-DIC pool up to 4.2
372 times higher than the DIC concentrations of external seawater (Fig. 2d-LS). This
373 result supports carbon budget in internal symbiosis in Xu et al.[20] We further
374 discovered that the DIC pool remained when no external DIC was provided (Fig.

375 2d-DG/LG), showing that it does not depend on external seawater DIC and was more
376 associated with its metabolic CO_2 production. More interestingly, the DIC pool was
377 rarely consumed in the dark (Fig. 2d-DG/DS), which means although the calcification
378 consumes DIC, the coral hosts were unable to efficiently eliminate CO_2 without
379 symbiont photosynthesis. This result differs from the explanation that internal-DIC
380 pool in corals is used for photosynthesis and calcification[30,31,32], supporting the Furla
381 et al.[24] view that the host DIC is actively supplied to microalgal symbionts in a
382 light-dependent manner and not used as a source for calcification. In addition, we
383 found the significance of symbiont DIC removal to the host. The corals can
384 continuously consume external glucose only in the light (Fig. 2c-LG), whereas they
385 cannot sustainably utilize glucose in the dark (Fig. 2c-DG). Based on changes in the
386 host tissues DIC (Fig. 2d), we presumed that if there is no photosynthetic
387 consumption, the corals could not take up glucose when their internal-DIC reached a
388 certain threshold. Pogoreutz et al.[61] showed that the addition of sugar (including
389 glucose) readily attributed to a fourfold increase of coral-associated microbial nitrogen
390 fixation and then induced bleaching. In our experiment, the coral did not bleach during
391 8 days, but it is undeniable that further studies should consider the effects of N, P, etc.
392 more comprehensively. Since we know that the symbiont microalgae require high
393 levels of DIC for photosynthesis, the coral hosts, having a low DIC removal capacity,
394 accumulate DIC in the light seemingly a detrimental behaviour for themselves, but
395 actrually would be beneficial or even necessary to maintaining the
396 host-Symbiodiniaceae symbiosis.

397 Results from the transcriptome support and explain our hypothesis that the DIC pool
398 accumulated by corals may be the basis of symbiosis on a molecular level. Foremost,
399 we found that the coral have evolved several DIC enrichment pathways, and they
400 mainly serve the photosynthesis of the microalgae. Although several studies have
401 explored CCMs in coral hosts[20,62,63] and some of them proposed that the host's CAs
402 are involved in calcification[53,64], our results provide evidence that the host CAs do not
403 act primarily on their own calcification or emission of respiration CO_2, because they
404 have relatively low CAs activity in the dark compared to the light (Fig. 3a). The CAs
405 are most likely functioning to supply DIC to the microalgal photosynthesis. This fully
406 explains why coral hosts, having taken up enough DIC (Fig. 2d), continue to enrich
407 their quantities of it. More detailed CA annotation results indicate that coral
408 host-symbiont may possess different CA types with distinct functions and enhance
409 carbon synergistically (Fig. 3d). Similarly, Tansik et al.[65] also found that the supply of
410 DIC in the coral symbionts is usually under the control of the hosts. If that is true, there
411 may be other pathways that have evolved to "retain" the Symbiodiniaceae during coral
412 symbiosis that have not been discovered yet.
413 More interestingly, we have identified a potential carbon fixation pathway within coral
414 hosts that could supplement the CCMs, i.e., the PEPCK pathway. Notably, PEPCKase
415 can act as a carboxylase in invertebrates[66,67]. In natural conditions, when the
416 symbionts lacked DIC at the late stage, CAs activity gradually weakened while
417 PEPCKase activity gradually increased. At the same time, the gene expression of
418 three PEPCK sequences was significantly up-regulated (Fig. 3e-LS in red Gene ID),

419 which is different from the role played by PEPCK in gluconeogenesis (Fig. 3e-LS in
420 black Gene ID). In this process, PEPCKase may serve as PEPCase, converting PEP
421 into oxaloacetate, which efficiently concentrates DIC in the C_4 pathway, just as the
422 microalgal C_4 pathway has been reported[68,69,70]. There is another possibility that
423 oxaloacetate formation by PEPCKase replenishes the TCA cycle under increased
424 malate efflux, which accelerates tissue carbon flux to meet the photosynthetic
425 requirements of the microalgae. This mechanism bears similarities to the increasing
426 number of microalgal studies in recent years[71,72,73]. Notably, in the case of corals, the
427 hosts play a pivotal role in facilitating this step of carbon fixation for the symbiont.
428 Furthermore, CO_2 produced by host respiration is an important carbon source for
429 Symbiodiniaceae photosynthesis. When glucose is used as the only carbon source,
430 the hosts' glycolysis genes (purple arrows in Fig. 4c-LG) and TCA cycle genes (brown
431 arrows in Fig. 4c-LG) were up-regulated in the light, which showed that they were
432 uptaking glucose for metabolic needs to release by-product CO_2. These findings have
433 similarities with previous studies that heterotrophic feeding and glucose enrichment
434 can elevate the respiration rate of coral hosts, subsequently enhancing symbiont
435 photosynthetic rates[74,75]. What's more, the hosts must prevent more CO_2 production
436 without microalgal photosynthesis, i.e., by stopping the uptake of external glucose
437 and accelerating gluconeogenesis to meet its own metabolic needs (Fig. 4c-DG). All
438 the above corroborate our physiological indicators (Fig. 2cde-DG, LG).
439 Surprisingly, our results suggest that coral calcification is more likely to be a provider
440 of DIC to microalgal photosynthesis rather than a competitor for DIC. Previous

experiments shown that calcification is a competitor for photosynthesis, consuming 60% of the respiration-based CO_2[25,26]. In contrast, it has been argued that there is no competition, and calcification rates are higher under light conditions compared to darkness[27,28,29]. Numerous hypotheses have been proposed to explain the mechanisms behind light-enhanced calcification. The most widely supported hypothesis suggests that the photosynthetic metabolites produced by microalgae can supply ample nutrients for host growth, thereby accelerating the calcification process[76,77,78]. However, in our experiment, even with sufficient external nutrition, all coral calcification genes were down-regulated when exposed to darkness (Fig. 5-DG), and up-regulated or unchanged in the light (Fig. 5-LG), suggesting that the correlation between calcification and coral growth is not robust. This is consistent with experimental results under dark conditions where both HCO_3^- in external seawater and DIC in coral tissue remained utilized (Fig. 2b,d-DS), indicating that calcification may not be an actively-driven process. It can be inferred that coral calcification doesn't occur in tandem with host growth but is primarily fueled by the strong carbon demands of symbiotic organisms. The CO_2 released during calcification isn't promptly expelled from the coral body but is instead absorbed and utilized by Symbiodiniaceae, which may provide a new explanation for the controversial issue of the coral as a carbon source or carbon sink[79,80].

Finally, to confirm the significance of DIC in maintaining the coral-Symbiodiniaceae relationship, we performed 1% CO_2 gas dosing addition experiments to increase the DIC concentration by a factor of 1.2 times higher than the natural seawater. Notably,

463 compared to HCl addition group with the same pH, *G. lobata* and *A. digitifera* lost their
464 Symbiodiniaceae on day 12 and day 3, respectively (Fig. 6ab), suggesting it was high
465 CO_2 rather than low pH that caused the microalgae to depart from the coral.
466 Meanwhile, the microalgal loss rates were positively correlated with CO_2 solubility (Fig.
467 6bc), suggesting that the higher external CO_2 concentration was more attractive to the
468 microalgae. The enzymes associated with anti-oxidadation activities of corals were
469 not increased in CO_2 group (Fig. 6de), and more interestingly the detached
470 microalgae in seawater had higher CAs activity (Fig. 6h) and similar photosynthetic
471 efficiency (Fig. S3d,e) than those within corals. This suggests that the coral bleaching
472 in our experiments was not a result of the coral host expelling Symbiodiniaceae
473 because they were not functioning properly, but most likely a result of the microalgae
474 actively departing from the coral. From an evolutionary biology view, the microalgae's
475 behavior is paradoxical, implying that they actively abandon the protection of their
476 hosts. However, our experiments dramatically increased the CO_2 concentration in a
477 short time, which could have avoided the limitation of other nutrient factors and made
478 the microalgae respond more quickly. Another study found a similar phenomenon that
479 the increased CO_2 caused stress and reduced Symbiodiniaceae in *Galaxea*
480 *fascicularis* and caused bleaching[81]. Undeniably, there are many resources that
481 influence the coral-Symbiodiniaceae symbiosis[8,9,10,11], but our experiment provides
482 good evidence demonstrating the importance of actively DIC accumulation by the
483 hosts in maintaining coral symbiotic relationships, because once the external DIC
484 reaches concentrations sufficient for Symbiodiniaceae growth, the microalgal may

leave the host.

In summary, in this study, we provide a new perspective to understand the basis of coral symbiosis. We propose that the coral hosts may have complementary DIC utilization characteristics with Symbiodiniaceae and actively accumulate DIC for the symbiont microalgae. The internal-DIC in coral tissue is supplied to Symbiodiniaceae, not used for calcification. Coral hosts CCMs, respiration and calcification are all critical for the accumulation of DIC for microalgal photosynthesis, and there are even other possible carbon fixation pathways, i.e., PEPCK (Fig. S4). Furthermore, our hypothesis argues that the coral bleaching caused by heatwaves and acidification[82,83,84] may not be comprehensive, because it is also possible that as more greenhouse gases are incorporated into the ocean, it results in a situation where the hosts can no longer provide a relatively high CO_2 environment, and thus lose the attraction to the microalgae, resulting in the collapse of the symbiosis. This may provide a new perspective on coral bleaching under climate change. Undoubtedly, to confirm these hypotheses, further experimental efforts over extended periods are needed, as well as consideration of the interactions with other available nutrients.

Methods

Coral collection

The colonies of scleractinian corals (*G. lobata*) were collected in Dapeng Bay (22°59'N, 114°33'E), Shenzhen, People's Republic of China in September 2022. The coral colonies were collected at a water depth of ~5 m and divided into 5×2×2 cm^3 blocks using a Gryphon AquaSaw XL (American) and then were immediately

507 transported to the indoor aquaria facilities of the Marine Biological Laboratory
508 (22°59'N, 113°97'E) at the Tsinghua Shenzhen International Graduate School.
509 Groups of 10 corals were cultured in 120 L aquariums filled with artificial seawater
510 (salinity = 33‰, pH = 8.2, T = 23-24 °C, light/dark = 12 h/12 h, Illumination with
511 blue-dominated coral lamps in natural light, light intensity = 200 μmol $m^{-2}s^{-1}$). After
512 allowing the corals to acclimatise to the laboratory environments for one month, we
513 initiated our experiments.

514 **Symbiodiniaceae isolation**

515 Symbiodiniaceae (*Symbiodinium* sp.) were fresh isolated from the *G. lobata*. First, the
516 coral tentacles were clipped, and the microalgae were blown out repeatedly with a
517 pipette gun. Second, the microalgae pellet was resuspended in seawater and
518 centrifuged at 1000 g for 5 min at 20 °C. Third, the remaining host debris was
519 removed using differential gradient centrifugation (900 g for 5 min → 700 g for 5 min
520 → 650 g for 5 min at 20 °C)[85,86,87]. Finally, the microalgae pellet was centrifuged at
521 2000 g for 10 min at 20 °C and resuspended in F/2 medium, and then examined
522 through an inverted microscope (Primo Vert, Germany) at 40× magnification. Isolated
523 Symbiodiniaceae were enriched in F/2 medium for further experiments.

524 **Symbiodiniaceae carbon demand measurement**

525 The carbon demand of Symbiodiniaceae was evaluted following the description by
526 Wu et al.[40] The seawater used in the experiment was decarbonised by the method of
527 Yellowlees et al.[42] and then added with corresponding concentrations of bicarbonate
528 ($NaHCO_3$). In detail, the pH was first adjusted to 4.5 with 1 M HCl to convert all DIC to

529 CO_2. Then, CO_2 was removed by simultaneous aeration with N_2 and agitation for 1 h.
530 1 mM Tris was then added, after which the pH was adjusted to 8.2 with 1 M of NaOH
531 to ensure the pH stability. Different amounts of $NaHCO_3$ were added to 40 mL-sealed
532 headspace bottles containing 20 mL of artificial seawater medium as a carbon source,
533 resulting in a final HCO_3^- concentration of 2 mM, 4 mM, and 8 mM, respectively. An
534 aliquot of 2 mL of Symbiodiniaceae culture (about 5.6×10^6 cells mL^{-1}) was added to
535 each headspace bottle. Each dosage was triplicated independently. These
536 experiments were conducted with continuous illumination (blue light, 200 μmol $m^{-2}s^{-1}$)
537 at 23-24 °C[88], and pH was maintained at 8-8.5[89].
538 To ensure that DIC was the only variable and to exclude the effects of changes in N
539 and P concentrations and light on microalgal growth, the incubation period was 36 h
540 (Excluding other nutritional factors, i.e., N, P). To avoid CO_2 diffusion to the air, the
541 headspace bottles were sealed except during the sampling process, and a control
542 group with only 22 mL of the corresponding concentration of $NaHCO_3$ was added at
543 each treatment to serve as a blank for the changes of DIC concentrations.
544 The biomass and DIC concentration in solution were measured every 12 h. Cell
545 counts were performed with a hemocytometer under an inverted microscope (Primo
546 Vert, Germany). Cellular dry weight was calculated by drying the microalgae in an
547 oven at 55 °C for more than 24 h to keep cell weight constant. The standard curve
548 between the cell counts and dry weight was established by preliminary experiments
549 (Table. S2), and the dry weight of the biomass in this experiment was estimated based
550 on cell counts. DIC concentrations were measured using a total organic carbon

551 analyzer (Shimadzu, Japan), which detects dissolved CO_2, HCO_3^-, and CO_3^{2-} in
552 solution. The average specific growth rate (g $L^{-1}d^{-1}$) over any two-time points was
553 obtained by the following equation:

554 $$\mu' = \frac{\ln N_2 - \ln N_1}{t_2 \quad t_1}$$

555 where N_2 and N_1 are the cell counts (g L^{-1}) at time t_2 and t_1, respectively.

556 **Coral absorbance of organic and inorganic carbon under different light**
557 **conditions**

558 These experiments were carried out under two different light conditions: light
559 (light/dark = 12 h/12 h, 200 μmol $m^{-2}s^{-1}$) and dark (continuous darkness), with or
560 without organic carbon. Here, organic carbon is defined as decarbonised seawater
561 with glucose (initial concentration of glucose 0.10 g L^{-1} based on the preliminary
562 experiment) as the only carbon source, whereas inorganic carbon is defined as
563 normal seawater with HCO_3^- (initial concentration of HCO_3^- 0.26 g L^{-1}) as the main
564 carbon source.

565 In total, four experimental treatments were set: DG (Continuous darkness and
566 glucose as the only carbon source), DS (Continuous darkness and $NaHCO_3$ as the
567 only carbon source), LG (12 h/12 h light/dark and glucose as the only carbon source),
568 and LS (12 h/12 h light/dark and $NaHCO_3$ as the only carbon source). Each coral was
569 cultured independently in 1.6 L of the respective medium. To exclude possible
570 interference from stored sugars, all corals used had been starved in darkness for 3
571 days before experiments. Triplicates of each treatment were conducted
572 independently.

573 During the experiment, coral visual changes were recorded every day using a camera
574 at fixed points, and quantified by the mean values of tentacle extension length using a
575 measuring ruler. The external DIC and glucose concentrations were detected
576 simultaneously. Whole coral tentacles were ground and homogenised, and then used
577 for measurements of carbon concentration and carbon fixation enzyme activities in
578 coral tissues every other day. On day 8 of this experiment, NO_3^- and PO_4^{3-} remained
579 in the medium.

580 **Coral bleaching induction by CO_2 gas exposure**

581 Two different species of scleractinian corals (*G. lobata* and *A. digitifera*) were selected
582 for the coral bleaching experiment. The experiments were set up with three
583 treatments: CO_2 group (1% CO_2 mixture gas was continuously aerated into seawater
584 at 0.05 L min^{-1}, with the microbubble plates generating microbubbles with an average
585 size of 400-600 μm, pH = 7.0), HCl group (1 M HCl was added to seawater daily to
586 adjust the same pH as the CO_2 group to examine the possible effect of changes pH on
587 the performance of coral, pH = 7.0) and control group (natural seawater, pH = 8.2),
588 and other conditions were kept the same (salinity = 33‰, T = 23-24 °C, light intensity
589 = 200 μmol $m^{-2}s^{-1}$, light/dark = 12 h/12 h). The same flow rate of air exposure did not
590 cause the Symbiodiniaceae to leave, which can exclude the effects of bubbles'
591 physical disturbance on corals. Each coral was placed in a 1.6 L system and cultured
592 independently. Each treatment was triplicated. During the experiment, the pH of
593 seawater and CO_2 solubility were measured daily. On the last day, free
594 Symbiodiniaceae were collected from seawater, and symbiotic microalgae on corals

595 were separated with water pick method. Meanwhile, the symbiotic microalgae
596 coverage, photosynthetic activity (Fv/Fm), chlorophyll, carbon fixation enzymes, and
597 anti-oxidative enzymes' activities were detected. The dissolved CO_2 were measured
598 using a total organic carbon analyzer (Shimadzu, Japan), and its relationship with
599 microbubble diameter was determined with the Planktonscope image system (Oasis
600 Photobio Tech, China).

601 **Physiological parameters and enzymatic activities**

602 DIC concentration in seawater was measured using a total organic carbon analyzer
603 (Shimadzu, Japan) with the Chinese standard of HJ 501-2009, and glucose
604 concentrations were measured by the dinitrosalicylic acid (DNS) method[90], DIC and
605 glucose consumption was calculated, respectively. A multi-excitation chlorophyll
606 fluorometer was used to measure the photosynthetic activity (Fv/Fm) of microalgal
607 cells. Chlorophyll was quantified using the methods of Ji et al.[91] and Laura et al.[92],
608 respectively. Protein concentrations were determined with the bicinchoninic acid (BCA)
609 method[93] for homogenisation of all assay metrics. The activities of carbon fixation
610 enzymes, i.e., CAs, PEPCase and PEPCKase, and anti-oxidative enzymes, i.e.,
611 SODase and CATase were measured by double antibody sandwich method using
612 ELISA kits (Thermo Fisher Scientific, USA).

613 **Transcriptomics analysis**

614 On day 8 of the coral culture experiments, all the corals were taken out and
615 fast-frozen with liquid nitrogen for transcriptomic analysis. Total RNA was extracted
616 using the Trizol-centrifugal column method, and then sent to the Shanghai Majorbio

617 Bio-pharm Technology Co., Ltd. (Shanghai, China) for the construction of an RNA-seq
618 transcriptome library. Each treatment was replicated three times. The data were
619 analyzed using the Majorbio Cloud online platform (https://www.majorbio.com/). Raw
620 reads were trimmed and quality controlled by fastp (Version 0.19.5).
621 To distinguish the sequences of coral and Symbiodiniaceae, the clean data from the
622 samples were used to do *de novo* assembly with Trinity (Version 2.8.5) initially, and all
623 the assembled sequencs were filtered by CD-Hit (Version 4.5.7) and TransRate
624 (Version 1.0.3) to increase quality. Species annotation was performed through the
625 NCBI-NR database to select coral species for subsequent analysis. Meanwhile, the
626 clean reads were aligned to reference genome of Symbiodiniaceae (*Cladocopium*
627 *goreaui*, http://sampgr.org.cn/index.php/download) with orientation mode using
628 HISAT2 (Version 2.1.0), and the alignment rates ranged from 31.23% to 36.9%. The
629 mapped reads were assembled by StringTie (Version 2.1.2).
630 The expression level of each transcript was calculated according to the transcripts per
631 million reads (TPM) method. DEGs between four treatments were identified using
632 DESeq2 (Version 1.24.0), and DEGs with $|\log_2 FC| \geq 1$ and P-value < 0.05 were
633 considered to be significantly different expressed genes. Subsequently, DIAMOND
634 (Version 0.9.24) was used to compare with the NCBI-NR database for species
635 annotation, and with the KEGG database for functional annotation (E-value $< 10^{-5}$,
636 identity ≥ 50%, and comparison length ≥ 50%). Metabolic pathways were mapped
637 using the KEGG Pathway as the primary reference. BLAST+ (Version 2.9.0) was used
638 to compare with KEGG, Swissprot, and Pfam databases to obtain more coding genes

639 and classification information of PEPC, PEPCK, and CA in the transcriptome.

640 **Statistical analysis and data availability**

641 All experiments were conducted with a minimum of three biological replicates to
642 ensure result reproducibility. The results are presented as mean ± standard deviation
643 (SD). Statistical analysis was performed using SPSS (Version 26.0) and R (Version
644 4.4.0). Statistical significance was determined at thresholds of 0.05. All tested growth
645 rates and activity indicators were analysed using two-way ANOVA, followed by
646 Tukey's HSD post-hoc analysis ($p < 0.05$). Genetic distances were calculated using
647 MEGA11 based on the P-distance model, and phylogenetic trees were constructed
648 using the Neighbor-Joining (NJ) method[94]. Heatmaps were drawn using ImageGP
649 (https://www.bic.ac.cn/ImageGP/) and Z-Score normalisation was performed.

650 **Data availability**

651 The data of this study are available within the article. Source data collected in this
652 study are available from Zenodo online (https://doi.org/10.5281/zenodo.11276136).
653 Raw RNAseq reads for differential gene expression analyses have been submitted to
654 NCBI's SRA database (http://www.ncbi.nlm.nih.gov) under BioProject PRJNA1115939.
655 The KEGG database (https://www.kegg.jp/) was used for functional enrichment
656 analyses.

657 **Code availability**

658 All scripts for data visualisation are available from Zenodo online
659 (https://doi.org/10.5281/zenodo.11276136).

660 **References**

661 1. Shi, T., Zheng, X. Q., Zhang, H., Wang, Q. F. & Zhong, X. Coral reefs: potential
662 blue carbon sinks for climate change mitigation. *Bull. Chin. Acad. Sci.* **36**,
663 270-278 (2021).

664 2. Webb, K. L., DuPaul, W. D., Wiebe, W., Sottile, W. & Johannes, R. E. Enewetak
665 (Enewetok) atoll: aspects of the nitrogen cycle on a coral reef. *Limnol. Oceanogr.*
666 **20**, 198-210 (1975).

667 3. Dobson, K. L. et al. Moderate nutrient concentrations are not detrimental to corals
668 under future ocean conditions. *Mar. Biol.* **168**, 98 (2021).

669 4. Titlyanov, E. & Titlyanova, T. Reef-building corals-symbiotic autotrophic
670 organisms: 1. general structure, feeding pattern, and light-dependent distribution
671 in the shelf. *Russ. J. Mar. Biol.* **28**, 1-15 (2002).

672 5. Wooldridge, S. A. A hypothesis linking sub-optimal seawater pCO_2 conditions for
673 cnidarian-*Symbiodinium* symbioses with the exceedence of the interglacial
674 threshold (>260 ppmv). *Biogeosciences* **9**, 1709-1723 (2012).

675 6. Muller-Parker, G., D'elia, C. F. & Cook, C. B. Interactions between corals and their
676 symbiotic algae. *Coral Reefs Anthropocene*, 99-116 (2015).

677 7. LaJeunesse, T. C. et al. Systematic revision of Symbiodiniaceae highlights the
678 antiquity and diversity of coral endosymbionts. *Curr. Biol.* **28**, 2570-2580 (2018).

679 8. Rädecker, N., Pogoreutz, C., Voolstra, C. R., Wiedenmann, J. & Christian, W.
680 Nitrogen cycling in corals: the key to understanding holobiont functioning? *Trends*
681 *Microbiol.* **23**, 490-497 (2015).

682 9. Ferrier-Pagès, C., Godinot, C., D'angelo, C., Wiedenmann, J. & Grover, R.
683 Phosphorus metabolism of reef organisms with algal symbionts. *Ecol. Monogr.* **86**,
684 262-277 (2016).
685 10. Ferrier-Pagès, C. et al. Symbiotic stony and soft corals: Is their host-algae
686 relationship really mutualistic at lower mesophotic reefs? *Limnol. Oceanogr.* **67**,
687 261-271 (2022).
688 11. Wiedenmann, J. et al. Reef-building corals farm and feed on their photosynthetic
689 symbionts. *Nature* **620**, 1018-1024 (2023).
690 12. Falkowski, P. G., Dubinsky, Z., Muscatine, L. & Porter, J. W. Light and the
691 bioenergetics of a symbiotic coral. *Bioscience* **34**, 705-709 (1984).
692 13. Treignier, C., Grover, R., Ferrier-Pagès, C. & Tolosa, I. Effect of light and feeding
693 on the fatty acid and sterol composition of zooxanthellae and host tissue isolated
694 from the scleractinian coral *Turbinaria reniformis*. *Limnol. Oceanogr.* **53**,
695 2702-2710 (2008).
696 14. Ferrier-Pagès, C. et al. Tracing the trophic plasticity of the coral-dinoflagellate
697 symbiosis using amino acid compound-specific stable isotope analysis.
698 *Microorganisms* **9**, 182 (2021).
699 15. Whitney, S. M., Shaw, C. & Yellowlees, D. Evidence that some dinoflagellates
700 contain a ribulose-1, 5-bisphosphate carboxylase/oxygenase related to that of the
701 α-proteobacteria. *Proc. R. Soc. B* **259**, 271-275 (1995).
702 16. Raven, J. A., Suggett, D. J. & Giordano, M. Inorganic carbon concentrating
703 mechanisms in free-living and symbiotic dinoflagellates and chromerids. *J.*

704 *Phycol.* **56**, 1377-1397 (2020).

705 17. Kumar, K. & Das, D. Carbon dioxide sequestration by biological processes.
706 In *Transformation and utilization of carbon dioxide*. Berlin, Heidelberg: Springer
707 Berlin Heidelberg. 303-334 (2014).

708 18. Allgeier, J. E. et al. Rewiring coral: Anthropogenic nutrients shift diverse
709 coral–symbiont nutrient and carbon interactions toward symbiotic algal
710 dominance. *Glob. Chang. Biol.* **26**, 5588-5601 (2020).

711 19. Roberty, S., Béraud, E., Grover, R., & Ferrier-Pagès, C. Coral productivity is
712 co-limited by bicarbonate and ammonium availability. *Microorganisms* **8**, 640
713 (2020).

714 20. Xu, Y. et al. Coral symbiosis carbon flow: a numerical model study spanning
715 cellular to ecosystem levels. *Front. Mar. Sci.* **9**, 749921 (2022).

716 21. Muscatine, L., Porter, J. W., & Kaplan, I. R. Resource partitioning by reef corals
717 as determined from stable isotope composition: I. δ ^{13}C of zooxanthellae and
718 animal tissue vs depth. *Mar. Biol.* **100**, 185-193 (1989).

719 22. Rädecker, N., Pogoreutz, C., Wild, C., & Voolstra, C. R. Stimulated respiration
720 and net photosynthesis in *Cassiopeia* sp. during glucose enrichment suggests in
721 hospite CO_2 limitation of algal endosymbionts. *Front. Mar. Sci*. **4**, 267 (2017).

722 23. Al-horani, F. A., Al-mogherabib, S. M. & Beera, D. E. Microsensor study of
723 photosynthesis and calcification in the scleractinian coral, *Galaxea fascicularis*:
724 active internal carbon cycle. *J. Exp. Mar. Biol. Ecol.* **288**, 1-15 (2003).

725 24. Furla, P., Galgani, I., Durand, I., & Allemand, D. Sources and mechanisms of

726 inorganic carbon transport for coral calcification and photosynthesis. *J. Exp. Biol.*
727 **203**, 3445-3457 (2000).
728 25. Langdon, C. & Atkinson, M. J. Effect of elevated pCO_2 on photosynthesis and
729 calcification of corals and interactions with seasonal change in
730 temperature/irradiance and nutrient enrichment. *J. Geophys. Res.* **110**, C09S07
731 (2005).
732 26. Uthicke, S. & Fabricius, K. E. Productivity gains do not compensate for reduced
733 calcification under near-future ocean acidification in the photosynthetic benthic
734 foraminifer species *Marginopora vertebralis*. *Glob. Change Biol.* **18**, 2781-2791
735 (2012).
736 27. Moya, A. et al. Carbonic anhydrase in the scleractinian coral *Stylophora pistillata*.
737 *J. Biol. Chem.* **283**, 25475 (2008).
738 28. Tambutte, S. et al. Coral biomineralization: from the gene to the environment. *J.*
739 *Exp. Mar. Biol. Ecol.* **408**, 58-78 (2011).
740 29. Inoue, M. et al. A simple role of coral-algal symbiosis in coral calcification based
741 on multiple geochemical tracers. *Geochim. Cosmochim. Ac.* **235**, 76-88 (2018).
742 30. Allison, N., Cohen, I., Finch, A. A., Erez, J. & Tudhope, A. W. Corals concentrate
743 dissolved inorganic carbon to facilitate calcification. *Nat. Commun.* **5**, 5741
744 (2014).
745 31. McCulloch, M. T., D'Olivo, J. P., Falter, J., Holcomb, M., & Trotter, J. A. Coral
746 calcification in a changing world and the interactive dynamics of pH and DIC
747 upregulation. *Nat. Commun.* **8**, 15686 (2017).

32. De Goeyse, S., Webb, A. E., Reichart, G. J. & De Nooijer, L. J. Carbonic anhydrase is involved in calcification by the benthic foraminifer *Amphistegina lessonii*. *Biogeosciences* **18**, 393-401 (2021).

33. Herfort, L., Thake, B., & Taubner, I. Bicarbonate stimulation of calcification and photosynthesis in two hermatypic corals. *J. Phycol.* **44**, 91-98 (2008).

34. Klein, S. G. et al. Symbiodinium mitigate the combined effects of hypoxia and acidification on a non-calcifying organism. *Glob. Chang. Biol.* **23**, 3690-3703 (2017).

35. Palardy, J. E., Grottoli, A. G. & Matthews, K. Effects of upwelling, depth, morphology and polyp size on feeding in three species of *Panamanian* corals. *Mar. Ecol. Prog. Ser.* **300**, 79-89 (2005).

36. Palardy, J. E., Rodrigues, L. J. & Grottoli, A. G. The importance of zooplankton to the daily metabolic carbon requirements of healthy and bleached corals at two depths. *J. Exp. Mar. Biol. Ecol.* **367**, 180-188 (2008).

37. Yasuda, N. et al. Genetic structure of the *Goniopora lobata* and *G. djiboutiensis* species complex is better explained by oceanography than by morphological characteristics. *Front. Mar. Sci.* **8**, 592608 (2021).

38. Sydney, E. B. et al. Potential carbon dioxide fifixation by industrially important microalgae. *Bioresour. Technol.* **101**, 5892-6 (2010).

39. Singh, S. P. & Singh, P. Effect of CO_2 concentration on algal growth: a review. Renew. Sustain. *Energy Rev.* **38**,172-179 (2014).

40. Wu, K. et al. Optimizing the growth of *Haematococcus pluvialis* based on a novel

770 microbubble-driven photobioreactor. *Iscience* **24**, 103461 (2021).

771 41. Powers, L. C., Brandes, J. A., Stubbins, A. & Miller, W. L. MoDIE: Moderate
772 dissolved inorganic carbon (DI^{13}C) isotope enrichment for improved evaluation of
773 DIC photochemical production in natural waters. *Mar. Chem.* **194**, 1-9 (2017).

774 42. Yellowlees, D. et al. Role of carbonic anhydrase in the supply of inorganic carbon
775 to the giant clam-zooxanthellate symbiosis. *Mar. Biol.* **115**, 605-611 (1993).

776 43. Moroney, J. V., Bartlett, S. G. & Samulesson, G. Carbonic anhydrases in plants
777 and algae. *Plant Cell Environ.* **24**, 141-153 (2001).

778 44. Field, D., Tiwari, B. & Snape, J. Bioinformatics and data management support for
779 environmental genomics. *PLoS Biol.* **3**, 1352-1353 (2005).

780 45. Heyduk, K., Moreno-Villena, J. J., Gilman, I. S., Christin, P. A. & Edwards, E. J.
781 The genetics of convergent evolution: insights from plant photosynthesis. *Nat.*
782 *Rev. Genet.* **20**, 485-493 (2019).

783 46. O'Leary, B., Park, J. & Plaxton, W. C. The remarkable diversity of plant PEPC
784 (phosphoenolpyruvate carboxylase): recent insights into the physiological
785 functions and post-translational controls of non-photosynthetic PEPCs. *Biochem.*
786 *J.* **436**, 15-34 (2011).

787 47. Koendjbiharie, J. G., van Kranenburg, R. & Kengen, S. W. M. The
788 PEP-pyruvate-oxaloacetate node: variation at the heart of metabolism. *FEMS*
789 *Microbiol. Rev.* **45**, fuaa061 (2021).

790 48. Liu, Y. Q., Tang, S., Yan, Q., Zhou, J. & Cai, Z. H. Effectiveness and associated
791 mechanisms of a combination of biofilm attached cultivation and mixotrophy in

792 promoting microalgal biomass. *Bioresour. Technol.* **393**, 130077 (2024).

793 49. Windhagauer, M. et al. Metabolic response to a heterologous
794 poly-3-hydroxybutyrate (PHB) pathway in *Phaeodactylum tricornutum*. *Appl.*
795 *Microbiol. Biotechnol.* **108**, 1-16 (2024).

796 50. Legouis, D., Faivre, A., Cippà, P. E. & de Seigneux, S. Renal gluconeogenesis:
797 an underestimated role of the kidney in systemic glucose metabolism. *Nephrol.*
798 *Dial. Transplant.* **37**, 1417-1425 (2022).

799 51. Weis, V. M. & Allemand, D. What determines coral health? *Science* **324**,
800 1153-1155 (2009).

801 52. Tohse, H., Murayama, E., Ohira, T., Takagi, Y. & Nagasawa, H. Localization and
802 diurnal variations of carbonic anhydrase mRNA expression in the inner ear of the
803 rainbow trout *Oncorhynchus mykiss*. *Comp. Biochem. Physiol. Part B: Biochem.*
804 *Mol. Biol.* **145**, 257-264 (2006).

805 53. Allemand, D., Tambutté, É., Zoccola, D. & Tambutté, S. Coral calcification, cells to
806 reefs. *Coral Reefs: an Ecosystem in Transition*, 119-150 (2011).

807 54. Fukuda, I. et al. Molecular cloning of a cDNA encoding a soluble protein in the
808 coral exoskeleton. Biochem. *Biophys. Res. Commun.* **304**, 11-17 (2003).

809 55. Sunagawa, S., DeSalvo, M. K., Voolstra, C. R., Reyes-Bermudez, A. & Medina, M.
810 Identifification and gene expression analysis of a taxonomically restricted
811 cysteine-rich protein family in reef-building corals. *PLoS One* **4**, e4865 (2009).

812 56. Grasso, L. C. et al. The biology of coral metamorphosis: molecular responses of
813 larvae to inducers of settlement and metamorphosis. *Dev. Biol.* **353**, 411-419

814 (2011).

815 57. Mass, T. et al. Cloning and characterization of four novel coral acid-rich proteins
816 that precipitate carbonates in vitro. *Curr. Biol.* **23**, 1126-1131 (2013).

817 58. Wang, X. et al. The evolution of calcification in reef-building corals. *Mol. Biol. Evol.*
818 **38**, 3543-3555 (2021).

819 59. Goldberg, W. M. Coral food, feeding, nutrition, and secretion: a review. *Mar.*
820 *Organisms as Model Systems in Biology and Medicine*, 377-421 (2018).

821 60. Cui, G. et al. Molecular insights into the *Darwin paradox* of coral reefs from the
822 sea anemone *Aiptasia*. *Sci. Adv.* **9**, eadf7108 (2023).

823 61. Pogoreutz, C. et al. Sugar enrichment provides evidence for a role of nitrogen
824 fixation in coral bleaching. *Glob. Chang. Biol.* **23**, 3838-3848 (2017).

825 62. Al-Moghrabi, S., Goiran, C., Allemand, D., Speziale, N., & Jaubert, J. Inorganic
826 carbon uptake for photosynthesis by the symbiotic coral-dinoflagellate
827 association ii. mechanisms for bicarbonate uptake. *J. Exp. Mar. Biol. Ecol.* **199**,
828 227-248 (1996).

829 63. Barott, K. L., Venn, A. A., Perez, S. O., Tambutté, S., & Tresguerres, M. Coral host
830 cells acidify symbiotic algal microenvironment to promote
831 photosynthesis. *PNAS* **112**, 607-612 (2015).

832 64. Bertucci, A. et al. Carbonic anhydrases in anthozoan corals-a review. *Bioorg. Med.*
833 *Chem.* **21**, 1437-1450 (2013).

834 65. Tansik, A. L., Fitt, W. K. & Hopkinson, B. M. Inorganic carbon is scarce for
835 symbionts in scleractinian corals. *Limnol. Oceanogr.* **62**, 2045-2055 (2017).

836 66. Fukuda, W., Fukui, T., Atomi, H. & Imanaka T. First characterization of an
837 archaeal GTP-dependent phosphoenolpyruvate carboxykinase from the
838 hyperthermophilic archaeon *Thermococcus kodakaraensis* KOD1. *J. Bacteriol.*
839 **186**, 4620-4627 (2004).
840 67. Allemand, D. & Furla, P. How does an animal behave like a plant? Physiological
841 and molecular adaptations of zooxanthellae and their hosts to symbiosis. *C. R.*
842 *Biol.* **341**, 276-280 (2018).
843 68. Mamedov, T. G. & Chollet, R. Discovery of novel phosphoenolpyruvate
844 carboxylase (PEPC) genes and their active polypeptides in the green microalga
845 *Chlamydomonas reinhardtii*. *Proc. ANAS (Biol. Sci.)* **65**, 99-105 (2010).
846 69. Wu, S. et al. Proteomic and biochemical responses to different concentrations of
847 CO_2 suggest the existence of multiple carbon metabolism strategies in
848 *Phaeodactylum tricornutum*. *Biotechnol. Biofuels* **14**, 1-17 (2021).
849 70. Kupriyanova, E. V., Pronina, N. A. & Los, D. A. Adapting from low to high: an
850 update to CO_2-concentrating mechanisms of *Cyanobacteria* and microalgae.
851 *Plants* **12**, 1569 (2023).
852 71. Seo, S., Jeon, H., Chang, K. S. & Jin, E. S. Enhanced biomass production by
853 *Phaeodactylum tricornutum* overexpressing phosphoenolpyruvate carboxylase.
854 *Algal Res.* **31**, 489-496 (2018).
855 72. Wei, L. et al. Transcriptomic and proteomic responses to very low CO_2 suggest
856 multiple carbon concentrating mechanisms in *Nannochloropsis oceanica*.
857 *Biotechnol. Biofuels* **12**, 1-21 (2019).

858 73. Wang, Y. et al. Realization process of microalgal biorefinery: the optional
859 approach toward carbon net-zero emission. *Sci. Total Environ.* 165546 (2023).
860 74. Rädecker, N., Pogoreutz, C., Wild, C. & Voolstra, C. R. Stimulated respiration and
861 net photosynthesis in *Cassiopeia* sp. during glucose enrichment suggests in
862 hospite CO_2 limitation of algal endosymbionts. *Front. Mar. Sci.* **4**, 267 (2017).
863 75. Lyndby, N. H. et al. Effect of feeding and thermal stress on photosynthesis,
864 respiration and the carbon budget of the scleractinian coral *Pocillopora*
865 *damicornis*. *bioRxiv* 378059 (2018).
866 76. Gladfelter, E. H., Michel, G. & Sanfelici, A. Metabolic gradients along a branch of
867 the reef coral *Acropora palmata*. *Bull. Mater. Sci.* **44**, 1166-1173 (1989).
868 77. Colombo-Pallotta, M. F., Rodríguez-Román, A. & Iglesias-Prieto, R. Calcification
869 in bleached and unbleached *Montastraea faveolata*: evaluating the role of oxygen
870 and glycerol. *Coral Reefs* **29**, 899-907 (2010).
871 78. Bertucci, A., Forêt, S., Ball, E. E. & Miller, D. J. Transcriptomic differences
872 between day and night in *Acropora millepora* provide new insights into metabolite
873 exchange and light-enhanced calcification in corals. *Mol. Ecol.* **24**, 4489-4504
874 (2015).
875 79. Van der Heijden, L. H. & Kamenos, N. A. Calculating the global contribution of
876 coralline algae to carbon burial. *Biogeosciences* **12**, 7845-7877 (2015).
877 80. Van Dam, B. R. et al. Calcification-driven CO_2 emissions exceed "Blue Carbon"
878 sequestration in a carbonate seagrass meadow. *Sci. Adv.* **7**, eabj1372 (2021).
879 81. Hii, Y. S., Ambok Bolong, A. M., Yang, T. T. & Liew, H. C. Effect of elevated carbon

880 dioxide on two scleractinian corals: *Porites cylindrica* (Dana, 1846) and *Galaxea*
881 *fascicularis* (Linnaeus, 1767). *J. Mar. Sci*. 2009.
882 82. Heron, S. F., Maynard, J. A., van Hooidonk, R. & Eakin C. M. Warming trends and
883 bleaching stress of the world's coral reefs 1985-2012. *Sci. Rep.* **6**, 38402 (2016).
884 83. Hughes, T. P. et al. Global warming and recurrent mass bleaching of corals.
885 *Nature* **543**, 373-377 (2017).
886 84. Dove, S. G., Brown, K. T., Van Den Heuvel, A., Chai, A. & Hoegh-Guldberg, O.
887 Ocean warming and acidification uncouple calcification from calcifier biomass
888 which accelerates coral reef decline. *Commun. Earth Environ.* **1**, 55 (2020).
889 85. Treignier, C., Tolosa, I., Grover, R., Reynaud, S. & Ferrier-Pagé sa, C. Carbon
890 isotope composition of fatty acids and sterols in the scleractinian coral *Turbinaria*
891 *reniformis*: effect of light and feeding. Limnol. Oceanogr. **54**, 1933-1940 (2009).
892 86. Ferrier-Pages, C. et al. Summer autotrophy and winter heterotrophy in the
893 temperate symbiotic coral *Cladocora caespitosa*. *Limnol. Oceanogr.* **56**,
894 1429-1438 (2011).
895 87. Imbs, A. B., Yakovleva, I. M., Dautova, T. N., Bui, L. H. & Jones, P. Diversity of
896 fatty acid composition of symbiotic dinoflagellates in corals: evidence for the
897 transfer of host PUFAs to the symbionts. *Phytochemistry* **101**, 76-82 (2014).
898 88. Gohari, M. Y. & Darki, B. Z. Physiological and biochemical responses of
899 dinoflagellate *Symbiodinium* sp. to the different light intensities. *Shahid Beheshti*
900 *Univ.* **4**, 524-533 (2020).
901 89. Søderberg, L. M. & Hansen, P. J. Growth limitation due to high pH and low

902 inorganic carbon concentrations in temperate species of the dinoflagellate genus
903 *Ceratium*. *Mar. Ecol. Prog. Ser.* **351**, 103-112 (2007).
904 90. Puspasari, F. et al. Characteristics of raw starch degrading α-amylase from
905 *Bacillus aquimaris* MKSC 6.2 associated with soft coral *Sinularia* sp. *Starch -*
906 *Stärke* **63**, 461-467 (2011).
907 91. Ji, M. K. et al. Biodegradation of bisphenol A by the freshwater microalgae
908 *Chlamydomonas mexicana* and *Chlorella vulgaris*. *Ecol. Eng.* **73**, 260-269
909 (2014).
910 92. Mydlarz, L. D. & Jacobs, R. S. An inducible release of reactive oxygen radicals in
911 four species of gorgonian corals. *Mar. Freshw. Behav. Physiol.* **39**, 143-152
912 (2006).
913 93. Rädecker, N. et al. Nutrient stress arrests tentacle growth in the coral model
914 *Aiptasia*. *Symbiosis* **78**, 61-64 (2019).
915 94. Koichiro, T., Glen, S. & Sudhir, K. MEGA11: molecular evolutionary genetics
916 analysis version 11. *Mol. Biol. Evol.* **7**, 3022-3027 (2021).

Acknowledgements

This work was supported by the Projects of Shenzhen Science and Technology Program（KCXFZ20211020163557022, KCXFZ20211020165547011), and the Cross Research and Innovation Funding of Tsinghua SIGS (JC2022004).

Author contributions

BY.Z. and ZH.C. conceptualised and designed the experiments. BY.Z., L.L., MT.X., YQ.L. and WM.X. performed the experiments. BY.Z., S.T. and JM.Z. analysed and visualised the data. BY.Z. and S.T. interpreted the results and wrote the manuscript. HS.B., J.Z., M.C.B. and ZH.C. revised the manuscript.

Competing interests

The authors declare no competing interests.

928 **Supplementary Information**

929 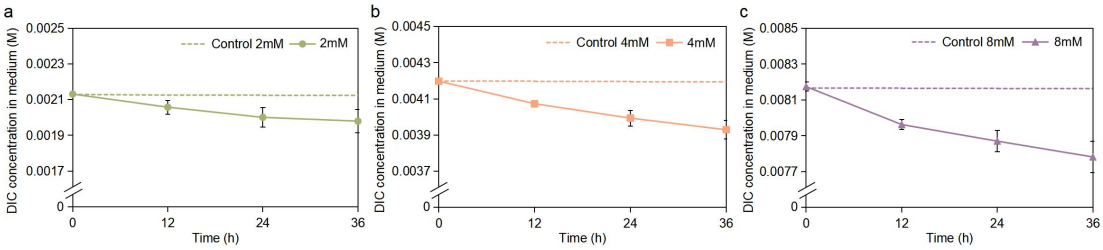

930 **Fig. S1: DIC consumption of monocultured Symbiodiniaceae at different carbon**

931 **concentrations. a-c**, DIC concentration in medium at 2 mM, 4 mM and 8 mM

932 $NaHCO_3$ group. The graphs show the mean ± SD (n = 3).

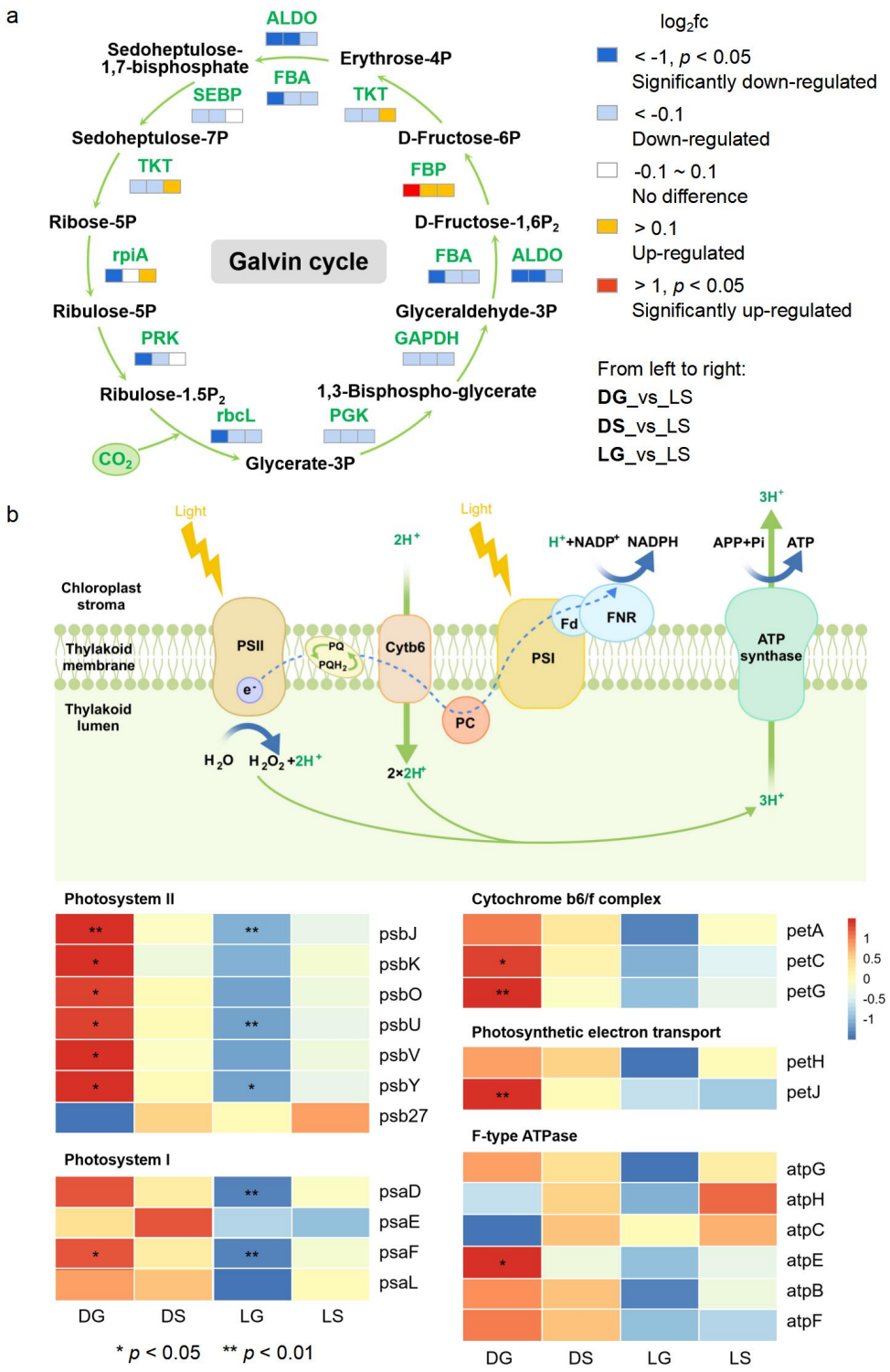

933

934 **Fig. S2: Comparison of the differential expression of photosynthesis genes in**

935 **Symbiodiniaceae. a,** Carbon fixation genes in Symbiodiniaceae. P_2 bisphosphate. P

936 phosphate. **b,** Photosynthesis photosystem genes in Symbiodiniaceae. The

937 expression results of one sequence with the largest length of the transcriptome

938 compared with the reference sequence of KEGG database were selected for each
939 gene in the figure. The colors indicate the log_2fc values of each treatment group
940 compared to the control LS, from left to right once for DG, DS, and LG. Heatmap
941 colors indicate relative expression levels, also the log_2fc values of each treatment
942 group compared with the control LS. P indicates the significance of the difference
943 between each treatment group and LS.

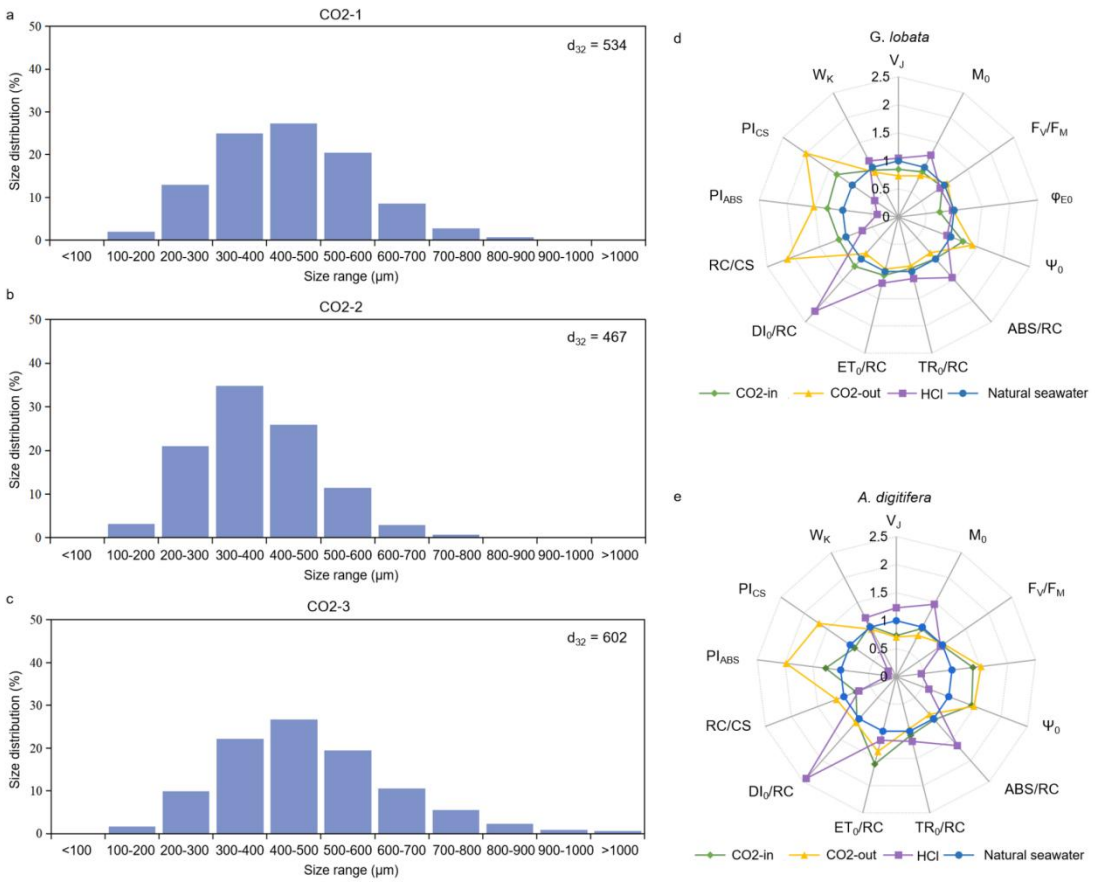

Fig. S3: Size range of microbubbles in CO_2 group and Chlorophyll fluorescence parameters of *G. lobata* and *A. digitifera*. a-c, Size range of microbubbles in CO_2 group 1-3. d_{32} indicate the diameters of microbubbles. **d-e**, Chlorophyll fluorescence parameters of *G. lobata* and *A. digitifera*, respectively. The related parameters used in chlorophyll fluorescence quantification were shown in Table. S1.

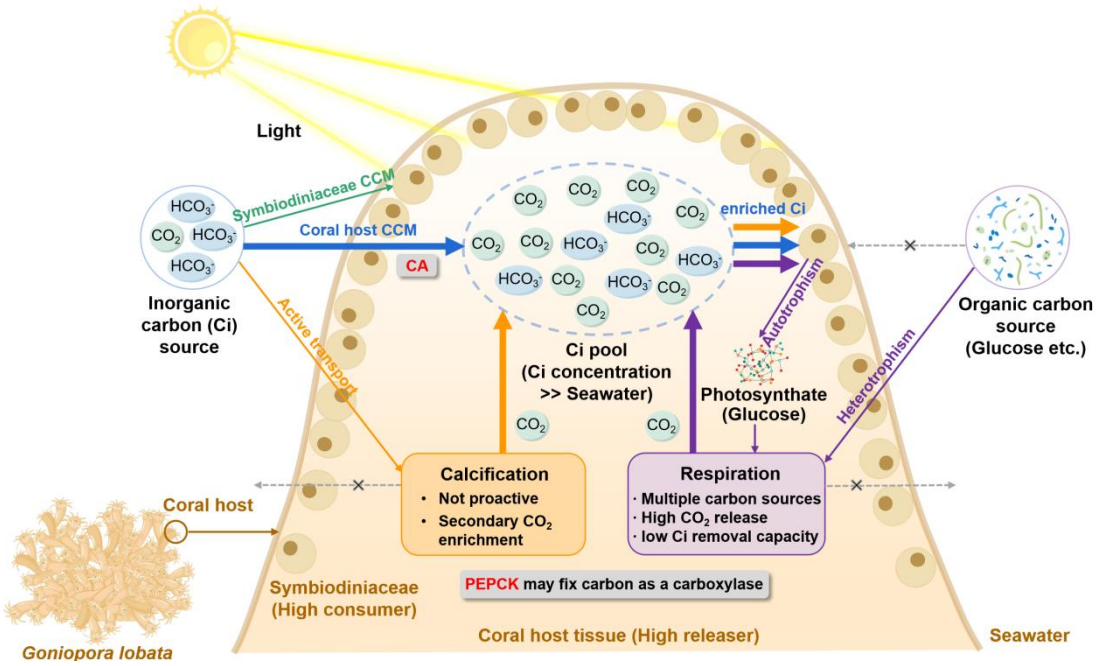

Fig. S4: Schematic diagram of the carbon fixation pattern of coral host-Symbiodiniaceae symbiosis. The diagram indicates the internal tissue in one tentacle of the *G. lobata*. Arrow colors indicate different DIC pathways. Green indicates symbiotic algal CCM. Blue indicates host CCM. Yellow indicates host calcification. Purple indicates host respiration.

Parameters & Formula	Description
$V_J=(F_{2ms}-F_0) / (F_m-F_0)$	Relative variable fluorescence intensity at the J-step
$M_0=4(F_{300\mu s}-F_0) / (F_m-F_0)$	The rate at which QA is reduced
$F_V/F_m=1-(F_0/F_m)=\varphi_{p0}$	Maximum photochemical efficiency (at t=0)
$\varphi_{E0}=ET_0/ABS=[1-(F_0/F_m)]\ \Psi_0$	Quantum yield for electron transport (at t=0)
$\Psi_0=1-V_J$	Probability that a trapped exciton moves an electron into the electron transport chain beyond Q_A (at t=0)
$ABS/RC=M_0\ (1/V_J)\ (1/\varphi_{p0})$	Absorption flux per reaction center
$TR_0/RC=M_0\ (1/V_J)$	Trapped energy flux per reaction center for Q_A reduction (at t=0)
$ET_0/RC=M_0\ (1/V_J)\ \Psi_0$	Trapped energy flux per reaction center for electron transfer (at t=0)
$DI_0/RC=(ABS/RC)-(TR_0/RC)$	Dissipated energy flux per reaction center (at t=0)
$RC/CS=\varphi_{p0}\ (V_J/M_0)\ ABS/CS_0$	Density of per excited cross section
$PI_{ABS}=(RC/ABS)\ [\varphi_{p0}/(1-\varphi_{p0})]\ [\Psi_0/(1-\Psi_0)]$	Performance index based on absorbed light energy
$PI_{CS}=(RC/CS)\ [\varphi_{p0}/(1-\varphi_{p0})]\ [\Psi_0/(1-\Psi_0)]$	Performance index of light cross-section
$W_K=(F_k-F_0)/(F_J-F_0)$	The damage degree to the photosynthetic system

Table. S1: The related parameters, formula and related-descriptions used in chlorophyll fluorescence quantification.

	Group 1	Group 2	Group 3	Group 4	Group 5
Dry weight ($g\ mL^{-1}$)	0.0031	0.0032	0.0029	0.0031	0.0032
Cell counts ($cell\ mL^{-1}$)	7.64×10^{6}	7.80×10^{6}	7.50×10^{6}	7.60×10^{6}	7.68×10^{6}
Dry weight of individual cells ($g\ cell^{-1}$)	4.06×10^{-10}	4.10×10^{-10}	3.87×10^{-10}	4.08×10^{-10}	4.17×10^{-10}

Table. S2: Preliminary experiments to calculate the standard curve between the cell counts and dry weight of Symbiodiniaceae. Average = 4.05×10^{-10}, SD = 1.12×10^{-11}.